Table1. Analysis of the transmembrane (TM) regions of both the human TP and IP receptors. Analysis of the transmembrane (TM) regions of both the human TP and IP receptors using TM sequence prediction softwares. TM sequence prediction servers SPLIT, TMpred, TMHMM, and HMMTOP were used to analyze the TM regions of both human TP and IP receptors (1-4). To test the stringency of these servers in predicting GPCR TM regions, GPCRs with known protein structures (opsin, β_2-AR, β_1-AR and A_2A-AR) were included as controls. The TMHMM program (highlighted in bold) showed a high degree of specificity in predicting the TM regions of the GPCRs analyzed and the predicted loop regions were used in the design of the chimeric receptors.

RECEPTOR			ICL1 Amino acid sequence	ICL2 Amino acid sequence	ICL3 Amino acid sequence
OPSIN	Crystal structure (PDB 1U19)		65-71	140-149	225-240
	Algorithm	SPLIT	62-72	140-152	229-250
		TMPred	60-73	140-152	228-252
		TMHMM	62-73	134-152	225-253
		HMMTOP	72-83	142-161	231-261
β_1-AR	Crystal structure (PDB 2VT4)		39-46	112-124	207-254
	Algorithm	SPLIT	40-47	105-126	201-230
		TMPred	42-52	112-132	204-235
		TMHMM	38-57	118-129	199-230
		HMMTOP	41-52	110-133	201-234
β_2-AR	Crystal structure (PDB 2RH1)		61-66	137-146	231-263
	Algorithm	SPLIT	61-68	133-151	223-241
		TMPred	63-74	135-156	224-246
		TMHMM	59-69	130-149	221-242
		HMMTOP	62-73	134-155	224-246
A2A	Crystal structure (PDB 3EML)		49-55	122-132	220-240
	Algorithm	SPLIT	49-51	117-135	219-238
		TMPred	56-62	113-142	216--245
		TMHMM	47-58	114-135	213-242
		HMMTOP	54-63	121-142	219-246
TP	Algorithm	SPLIT	56-65	128-152	229-248
		TMPred	50-70	132-153	220-250
		TMHMM	**52-63**	**131-148**	**226-247**
		HMMTOP	53-66	133-156	228-251
IP	Algorithm	SPLIT	41-47	124-134	213-235
		TMPred	38-47	116-137	203-237
		TMHMM	**38-48**	**118-135**	**211-237**
		HMMTOP	41-50	114-137	205-237

1. Tusnady, G. E. & Simon, I. (2001) *Bioinformatics (Oxford, England)* 17, 849-850. 2. Juretic, D., Zoranic, L., & Zucic, D. (2002) *Journal of chemical information and computer sciences* 42, 620-632. 3. Hofmann, K. a. S., W (1993) *Biol. Chem. Hoppe-Seyler* 374, 166. 4. Krogh, A., Larsson, B., von Heijne, G., & Sonnhammer, E. L. (2001) *Journal of molecular biology* 305, 567-580.

Table 2. Potential intermolecular interactions within the TP-Gα peptide interface.

TP region	Atoms in TP receptor			Atoms in Gαq C-terminal peptide
	TP-WT (model)	TP-ICL2B-IP (model)	TP-ICL3B-IP (model)	
TM3 (cytoplasmic end) and ICL2	R136-NH2	R136-NE R136-NH2		E355-OE2 E355-O E355-O
TM5 (cytoplasmic end) and ICL3	H224-ND1 E230-OE1	V219-O E230-OE1	H224-ND1 V225-O Q252-OE1	N352-ND2 N352-N Y356-OH K354-O Y356-OH Y356-OH V359-O

Figure 1. Saturation binding assays of wild type (WT) TP and the chimeric receptors using the TP antagonist [^{3}H] SQ29, 548. Saturation assays with membrane bound WT-TP and the chimeric receptors were performed with different concentrations of [^{3}H] SQ 29, 548 (0.5 nM -20 nM). Specific binding was obtained by removing nonspecific binding from total binding observed. Binding of [^{3}H] SQ 29,548 in the presence of 10 µM SQ 29,548 was used as a measure of nonspecific binding. The data is from a minimum of three independent experiments, with each point in duplicate.

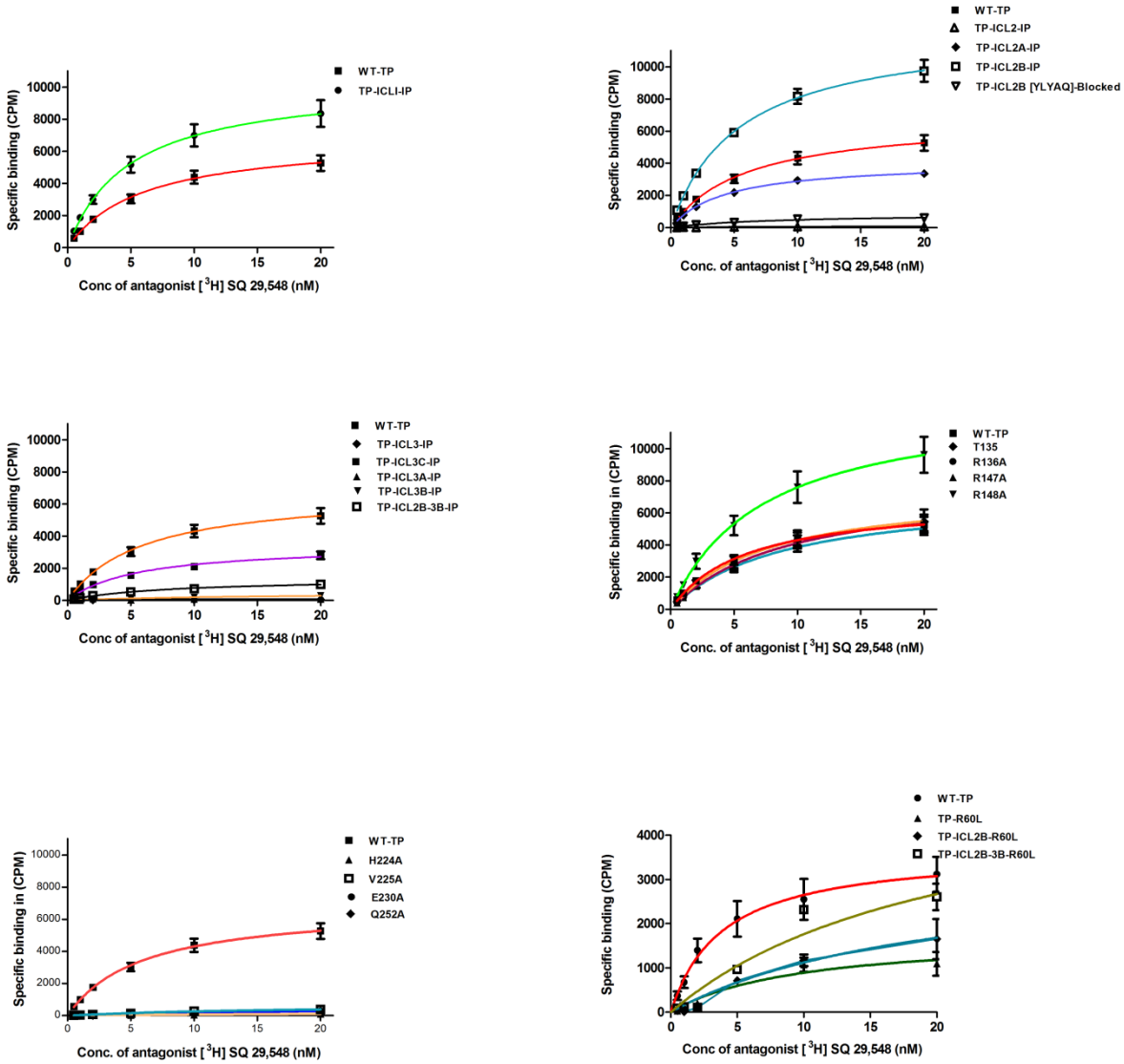

Figure 2. Immunofluorescence microscopy and western blot analysis of WT-TP and chimeric receptors in HEK293T cells. A) Double-label immunofluorescence was performed using mouse monoclonal anti-rho-1D4 antibody which recognizes the C-terminal octapeptide tag on the expressed receptors, and rabbit polyclonal anti-calnexin antibody which localizes to the endoplasmic reticulum (ER). The WT-TP and TP chimeric receptors were visualized using goat anti-mouse Alexafluor 488 secondary antibody (**panel A**) and the ER was visualized with goat anti-rabbit Alexafluor 594 secondary antibody (**panel B**). The nucleus stained with Hoechst-33342 dye is shown in blue (**panel C**). The overlay of the receptor, ER and nucleus is shown in **panel D** (location of the expressed receptor is indicated by an arrow). **B)** Western blot analysis was performed using 5µg of total solubilized membrane protein and the protein detected using monoclonal anti-rho-1D4 antibody, as described previously (2, 7). A representative blot is shown. Mol. wt range is indicated next to the gel. **C)** Agonist independent (untreated) and dependent (treated for 2hrs) internalization of TP, IP and TP-IP chimeras. FACS analysis to determine the receptors on the cell surface was performed using antibodies specific for the extracellular region of TP (and for TP-IP chimeras) and IP. TP and the chimeras were treated with the TP agonist U46619, while IP was treated with iloprost. The results are from two independent experiments in duplicate. Error bars represent mean ± SD.

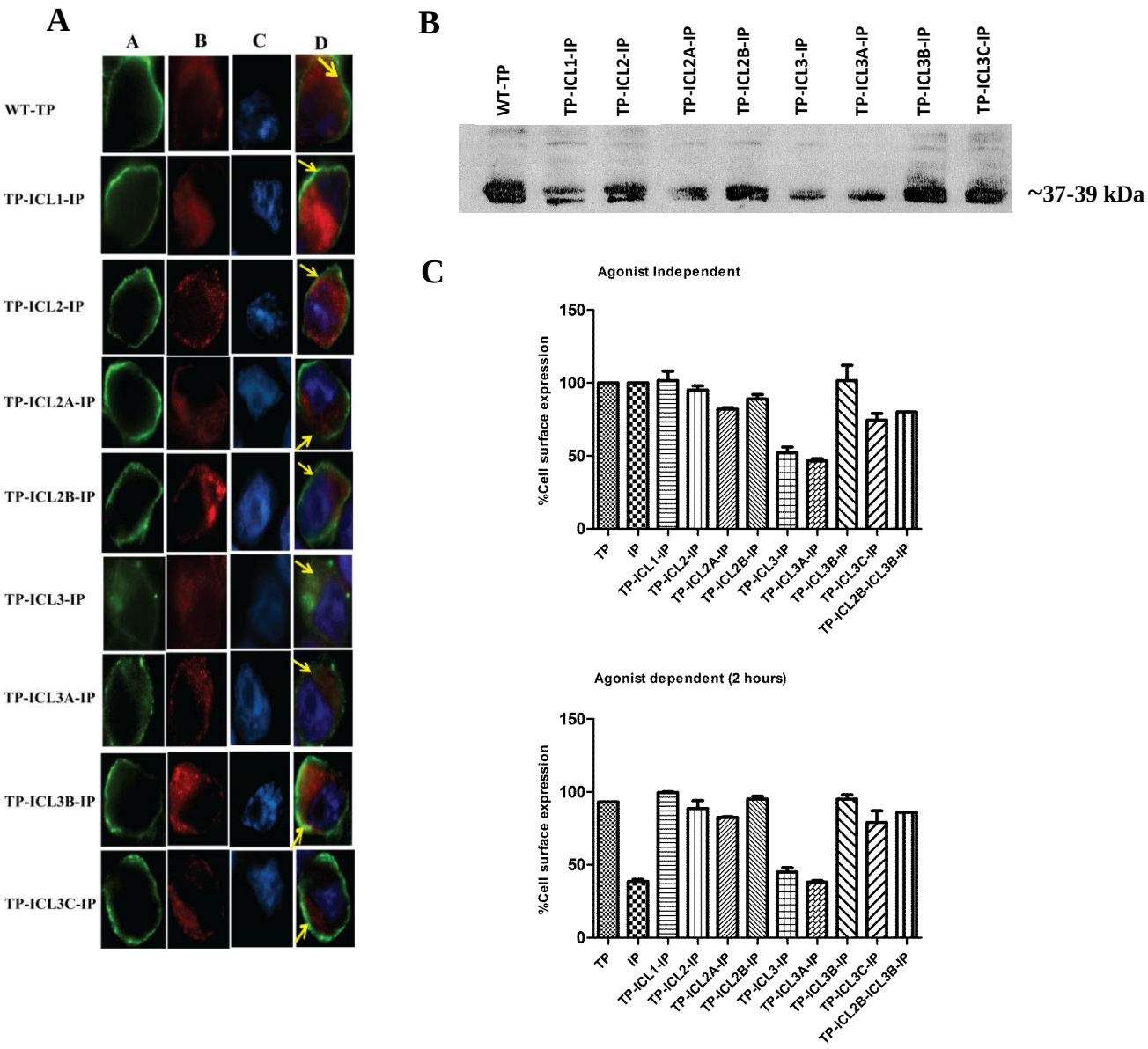

Figure 3. Analysis of IP_3 accumulation by WT-TP, WT-IP and chimeric receptors. A) IP_3 standard curve. An IP_3 standard curve was constructed by titrating known amounts of IP_3 and measuring the fluorescence according to instructions supplied by the manufacturer (HitHunter IP_3 assay kit, DiscoveRx, USA). The figure shows a linear relationship between the fluorescence measured (Y axis) with the amounts of IP_3 in picomoles (X axis). The slope value obtained ***y=-37.774x + 620.61*** was used to measure the amount of IP_3 released when cells expressing the receptors were treated with a single saturating concentration of agonist (10^{-6} M), and also the basal values without any agonist treatment. **B) IP_3 mobilized by WT and chimeric receptors.** Cells expressing the IP are stimulated with IP agonist Iloprost, while cells expressing the TP and TP-IP chimeras were stimulated with TP agonist U46619. Shown are the agonist-independent or basal activity (-), and activity after stimulation (+) with a single saturating concentration (1µM) of agonists to determine the maximal agonist-induced or intrinsic signal. Results are normalised to IP_3 mobilized by cell surface expression of the receptor as determined by FACS. Results are from a minimum of 3 independent experiments performed in duplicate. A one way ANNOVA with Tukeys *post hoc* test was used to check the significance level of the amount of IP_3 mobilized. The single asterisk indicate there is a significant difference in the amount of IP_3 mobilized at the highest concentration of agonist with respect to WT-IP at significance level of $p < 0.05$. Whereas double asterisk indicate IP_3 mobilization at basal level compared to WT-IP basal level activity and at significance level of $p < 0.05$.The bar plots does not include the chimeras TP-ICL3-IP, TP-ICL3A-IP as they failed to show any dose dependent response. Error bars represent mean ± SD.

A

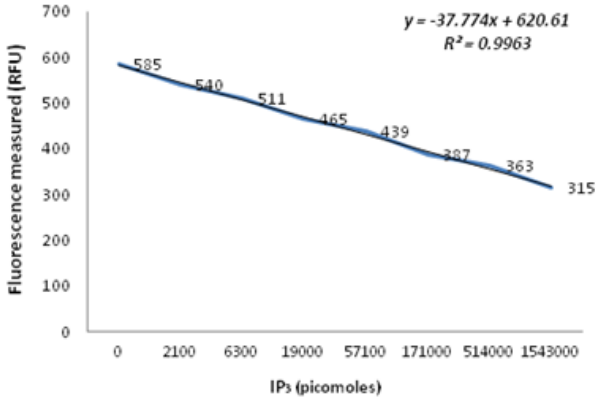

B

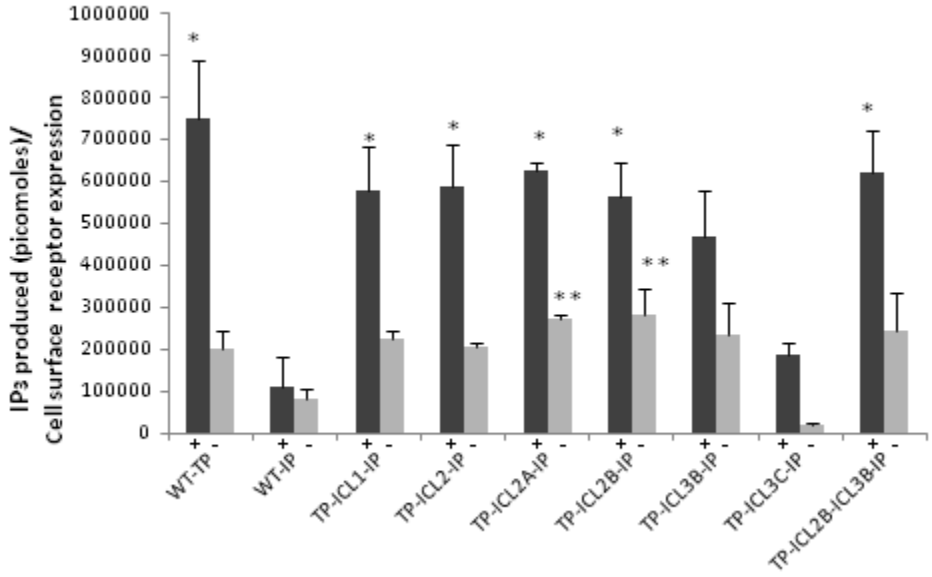

Figure 4. Characterization of Gαq mediated calcium signalling of the WT-TP, mutant receptors and chimeras containing the R60L variant. The data shows agonist U46619 induced calcium mobilization for WT-TP and mutants and normalized to wild type TP cell surface expression as determined by FACS. In panel A, ICL2 mutants; in panel B & C, ICL3 mutants and in panel D, the TP genetic variant R60L and the chimeras containing this genetic variant are displayed. TP-ICL2B-3B-IP-R60L rescues the signaling of the R60L to wild type TP levels (panel D).

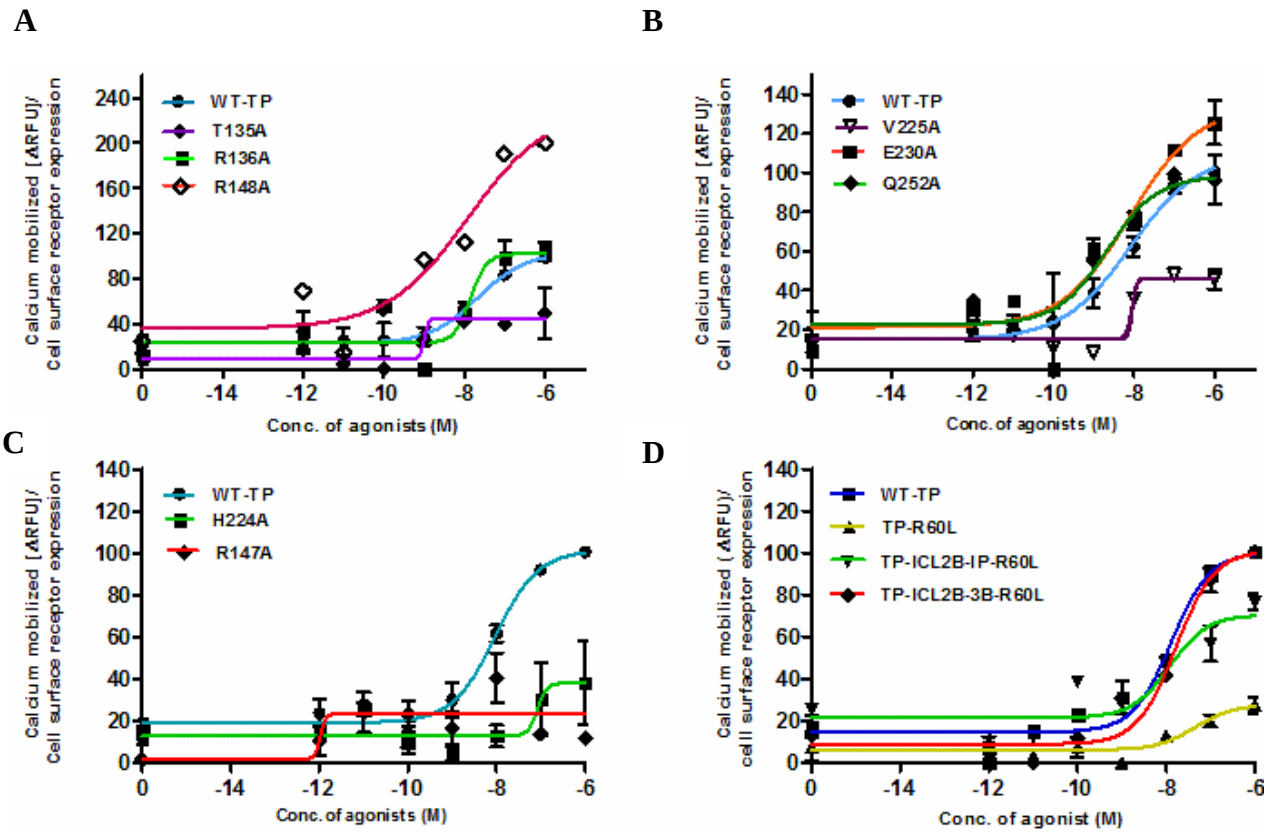

Figure 5. The bar plot represents the basal or agonist-independent calcium signaling by WT-TP, WT-IP, chimeric receptors and loop mutants. HEK293T cells expressing the WT-TP, WT-IP, loop mutants and the TP-IP chimeras are used in the assay. Shown are the agonist-independent or basal activity of these cells. Results are normalised to calcium mobilized by cell surface expression of the receptor as determined by FACS. Results are from a minimum of 3 independent experiments performed in duplicate. A one way ANNOVA with Tukeys *post hoc* test was used to check the significance level of the amount calcium mobilized. The double asterisk indicate there is a significant difference in the amount of calcium mobilized with respect to WT-IP receptor at significance level $p<0.05$. Error bars represent mean $\pm$ SD.

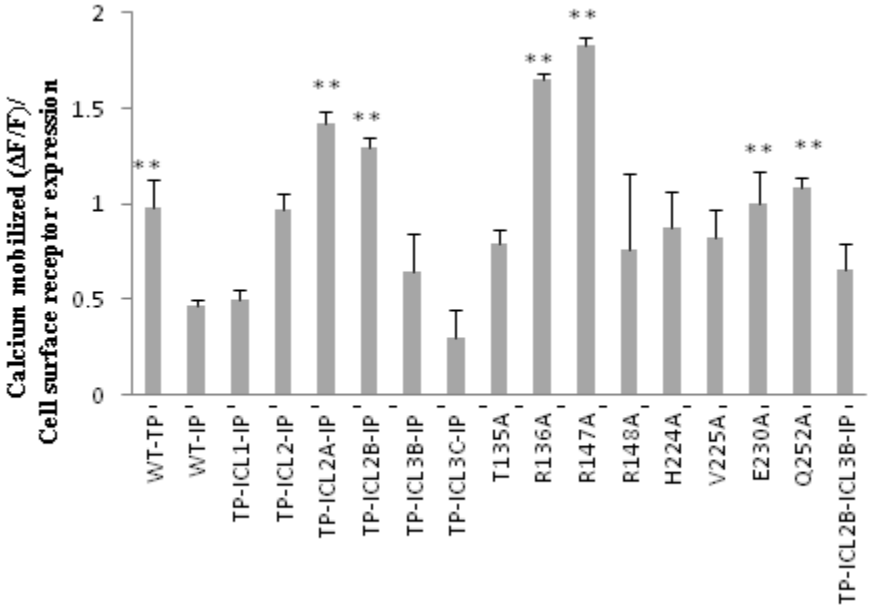

Figure 6: Amino acid sequence alignment of TP and IP (~27% homology), the ICL regions are highlighted in green. Except for the D/ERY motif present at the interface of TM3-ICL2, no additional Class A GPCR signature sequences are present in the ICL regions, of TP and IP.

```
TP    MWPNGSSLGPCFRPTNITLEERRLIASPWFAASFCVVGLASNLLALSVLAGARQGGSHTR
IP    ----------MADSCRNLTYVRGSVGPATSTLMFVAGVVGNGLALGILSARR---PARP
                 :  :  .*   *  ..*  :: : *.*:..* ***.:*:. *   .
TP    SSFLTFLCGLVLTDFLGLLVTGTIVVSQHAALFEWHAVDPG-CRLCRFMGVVMIFFGLSP
IP    SAFAVLVTGLAATDLLGTSFLSPAVFVAYARNSSLLGLARGGPALCDAFAFAMTFFGLAS
      *:* .:: **. **:**  . .. *.  :*   .  .:  *   **  :...* ****:.
TP    LLLGAAMASERYLGITRPFSRPAVASQRRAWATVGLVWAAALALGLLPLLGVGRYTVQYP
IP    MLILFAMAVERCLALSHPYLYAQLDGPRCARLALPAIYAFCVLFCALPLLGLGQHQQYCP
      :*:  *** ** *.:::*:  . : . * *  ::  ::* .: :  *****:*::    *
TP    GSWCFLTLG-AESGDVAFGLLFSMLGGLSVGLSFLLNTVSVATLCHVYHGQEAAQ-----
IP    GSWCFLRMRWAQPGGAAFSLAYAGLVALLVAAIFLCNGSVTLSLCRMYRQQKRHQGSLGP
      ****** :  *:.*..**.* :: * .* *.  ** *   . :**::*: *:  *
TP    -QRPRDSEVEMMAQLLGIMVVASVCWLPLLVFIAQTVLRNPPAMSPAGQLSRTTEKELLI
IP    RPRTGEDEVDHLILLALMTVVMAVCSLPLTIRCFTQAVAP----------DSSSEMGDLL
        *. :.**: :  *  : ** :** *** :     .:           . ::*   *:
TP    YLRVATWNQILDPWVYILFRRAVLRRLQPRLSTRPRSLSLQPQLTQRSGLQ---------
IP    AFRFYAFNPILDPWVFILFRKAVFQRLKLWVCCLCLGPAHGDSQTPLSQLASGRRDPRAP
       :*. ::* ******:****:**::**:  :.    . :   . *  * *
TP    ---------------------------------------------
IP    SAPVGKEGSCVPLSAWGEGQVEPLPPTQQSSGSAVGTSSKAEASVACSLC
```

Figure 7. Panel A, Molecular model of Gαq bound to TP predicted by superimposing the TP-Gαq 3D models on the β2AR-Gαs crystal structure followed by MD simulations for 10ns using SYBYLX v2.0. **Panel B**, represents a molecular model of Gαq C-terminal peptide bound to the TP predicted using Z dock server. In both the models, the Gαq C-terminal peptide is found bound between ICL2 and ICL3 regions. **Panel C**, In TP-wild type, R60 is interacting with M126 and R130 of ICL2 by H bond interactions, and the salt bridge between E129 of D/ERY motif and R148 is present. In case of TP-R60L mutant, interactions with M126 and R130 disappear but the salt bridge was still present, restraining the activity of the receptor.